Rapeseed protein concentrate as a potential ingredient for meat analogues

Wanqing Jia, Nicolas Curubeto, Elvira Rodríguez-Alonso, Julia K. Keppler, Atze Jan van der Goot [*]

Laboratory of Food Process Engineering, Wageningen University, PO Box 17, 6700 AA, Wageningen, the Netherlands

ABSTRACT

The potential for using rapeseed protein concentrate (RPC) as a novel protein source for meat analogues was investigated using shear cell technology with RPC-only and RPC-wheat gluten (WG) mixtures. The resulting products were characterized by texture analyser, confocal laser scanning microscopy (CLSM) and X-ray micro-tomography. Soy protein concentrate (SPC) was chosen as the benchmark because of its known capacity to create fibrous structures. Both RPC-only and RPC-WG mixtures could be transformed into fibrous products when processed at 140 °C and 150 °C with 40 wt% dry matter. The fibrous structure was improved by adding of WG into RPC at 140 °C and the colour of the RPC-WG product became lighter with more WG added. CLSM images revealed that the protein formed a continuous phase, and the RPC inherent polysaccharides acted as a dispersed phase. Overall, RPC is concluded as a promising alternative protein source after SPC for meat analogue applications.

Industrial relevance: Rapeseed meal, which is a by-product from extraction of rapeseed oil, is currently mainly used as animal feed and seldom applied as a food ingredient. This study provides valuable insights into the potential of rapeseed protein concentrate produced by washing rapeseed meal with aqueous ethanol as an alternative plant protein for meat analogues. The outcomes of this study demonstrated the potential of rapeseed protein concentrates for structuring purposes, which is a step towards its commercial use as an environmentally sustainable meat analogue ingredient.

1. Introduction

Plant-based meat analogues have received great interest from consumers who want to reduce their meat consumption. It is recognized that over-consumption of meat products is not only unhealthy but can also lead to environmental issues and ethical concerns about animal welfare. Shear cell technology has been reported to produce anisotropic fibrous meat analogues using (mixtures of) protein isolates or concentrates from soy, peas, wheat, and fababean (Dekkers, Nikiforidis, & van der Goot, 2016; Grabowska et al., 2016a; Grabowska, Tekidou, Boom, & van der Goot, 2014a; Schreuders et al., 2019). Plant-based meat analogues from sources such as legumes, oilseeds and cereals are gaining importance to address consumer demands and sustainability in future food supply. An important breakthrough would be the increased use of underutilized protein-rich by-products in meat analogue applications.

Rapeseed meal is a by-product obtained after oil extraction but it is seldom used for food applications. It has been suggested as an interesting alternative plant protein source due to its high protein content (35%–40%) and well-balanced amino acid profile (Tan, Mailer, Blanchard, & Agboola, 2011). In addition, favourable functionality has been reported with respect to emulsifying, gelling and oil/water binding properties (Asgar, Fazilah, Huda, Bhat, & Karim, 2010; Von Der Haar, Müller, Bader-Mittermaier, & Eisner, 2014; Wanasundara, 2011). The commercial value of this by-product would also increase significantly by making it suitable for application in meat analogues. Highly refined rapeseed protein isolates have been proposed as binders for meat products (Wanasundara, McIntosh, Perera, Withana-Gamage, & Mitra, 2016). A recent consumer study showed that the use of rapeseed protein as a main ingredient for meat analogues has gained consumer interest and attention (Banovic & Sveinsdóttir, 2021).

Table 1

Composition of RPC, SPC and WG, as well as the water holding capacity (WHC) and nitrogen solubility index (NSI).

Composition (% in dry base)	RPC	SPC	WG
Protein	55.9	73.9	79.4
Oil	2.2	2.1	NA
Ash	8.9	7.7	NA
Carbohydrate	33.6	21.9	12.61
Insoluble fibre	30.1	16.4	NA
Soluble fibre (pectin)	3.4	3.3	NA
Soluble sugars	0.1	2.2	NA
Functional properties			
WHC (g water/g dry pellet)	4.9 ± 0.4	6.3 ± 1.0	1.6 ± 0.03
NSI (%)	19.5 ± 0.7	42.9 ± 3.6	10.3 ± 3.9

NA, not applicable.

Table 2

Overview of the shear cell experiments with respect to the composition of RPC-only, SPC-only, RPC-WG mixtures and SPC-WG mixtures and the temperature applied in the shear cell.

Sheared sample	Composition (wt%)	T (°C)
RPC-only	40	25, 120, 130, 140, 150
RPC-WG mixtures	20–20	95, 120, 130, 140, 150
RPC-WG mixtures	32–8, 26–14, 20–20, 14–26, 8–32	140
WG-only	40	140
SPC-only	40	95, 120, 140
SPC-WG mixtures	20–20	

The formation of fibrous materials in shear cells is favoured when plant materials consist of two immiscible phases that deform and align upon shearing (Grabowska, Tekidou, Boom, & van der Goot, 2014b). Two immiscible phases can be achieved through mixing purified ingredients with different water holding capacities (WHCs) (i.e., soy protein isolate [SPI] and wheat gluten [WG]), or they can be present naturally in a single but less purified ingredient, such as soy protein concentrate (SPC) (i.e., proteins and polysaccharides). Rapeseed protein concentrate (RPC) is obtained from rapeseed meal after aqueous ethanol washing. As a result, the composition of RPC is similar to that of SPC in that it contains both proteins and polysaccharides (Wanasundara, 2011; Wanasundara et al., 2016). The polysaccharides mainly originate from the hulls and the cotyledon in rapeseed meal and are present as cellulose, hemicellulose and pectins. RPC has been studied in a shear cell before for fish feed to partially replace other plant protein sources, but at lower temperature than normally used to make fibrous materials. A solid, homogeneous material was obtained (Draganovic, Boom, Jonkers, & Van Der Goot, 2014). It showed potential to solidify, which is one of the requirements to become a suitable meat analogue ingredient.

Thus, the aim of this study was to investigate the structuring potential of RPC-only and RPC-WG mixtures for meat analogue production in a shear cell using different temperatures and ratios of RPC and WG. WG is often used in plant protein mixtures to enhance fibre formation in meat analogues (Cornet et al., 2021). The structural properties of the product was compared with that from SPC and an SPC-WG mixture by texture analyser using the uniaxial tensile test. The morphology of the structure was visualized by confocal laser scanning microscopy (CLSM). The air porosity of the sheared product was analysed by X-ray microtomography (XRT).

2. Materials and methods

2.1. Materials

RPC was provided by the Avril Group (France). Vital WG (Viten) was purchased from Roquette (Zaventem, Belgium). SPC (Alpha 8 IP; Solae Europe SA, Le Grand-Saconnex, Switzerland) was purchased from Dupont (Wilmington, DE, USA). NaCl was obtained from Sigma-Aldrich (Zwijndrecht, the Netherlands). Rhodamine B (Sigma R 6626; Sigma-Aldrich) and Calcofluor-white (Fluka, 18,909; Sigma-Aldrich) were used as staining agents for CLSM. The dry matter composition of RPC, SPC and WG is shown in Table 1; the composition of RPC was obtained from the Avril Group and the composition for SPC and WG is listed according to the manufacturer's specifications.

The WHC and nitrogen solubility index (NSI) were also measured, and the results are given in Table 1. The ability of the insoluble fraction to holding water was determined by adding 1 g of material and 49 g of Milli-Q water to a 50-mL Falcon tube, and rotated for 24 h in a rotator (Bibby Scientific Stuart Rotator Disk SB3, Thermo Fisher Scientific, Waltham, MA, USA) for hydration at a speed of 20 rpm. The dispersion was then centrifuged at a speed of 15,000 ×g at 25 °C for 10 min. The wet pellet was transferred into an aluminium tray and dried in the oven at 105 °C for 24 h. The nitrogen content in the dry pellet ($N_{dry\ pellet}$) and in the original sample ($N_{original}$) were measured with the Dumas combustion method using a nitrogen analyser (Flash EA 1112 Series; Thermo Scientific, Breda, the Netherlands). The mass of the original sample, wet pellet and dry pellet were obtained, denoted as $M_{original}$, $M_{wet\ pellet}$ and $M_{dry\ pellet}$. The WHC and NSI were calculated using eqs. (1,2).

$$\text{WHC} = \frac{M_{\text{wet pellet}} - M_{\text{dry pellet}}}{M_{\text{dry pellet}}} \ [\text{g water/g dry pellet}] \quad (1)$$

$$\text{NSI} = \frac{N_{\text{original}} \times M_{\text{original}} - N_{\text{dry pellet}} \times M_{\text{dry pellet}}}{N_{\text{original}} \times M_{\text{original}}} \ [\%] \quad (2)$$

2.2. Structure formation

2.2.1. Sample preparation

Aqueous dispersions of RPC, SPC, WG, RPC-WG mixtures, and SPC-WG mixtures were prepared and the compositions are listed in Table 2. Preliminary tests showed that a fibrous structure could be formed with RPC-only at 40 wt% dry matter. Therefore, 40 wt% was selected for all the tests in the paper, as well as 1 wt% sodium chloride, and 59 wt% demineralized water. For each experiment, samples with a total weight of 90 g were prepared as explained in the next section. Results with lower RPC concentrations are shown in Fig. S1. Samples were prepared by mixing sodium chloride with demineralized water in a

Table 3

Macrostructure of the sheared samples from RPC (40 wt%) and RPC-WG (20–20 wt%) from 120 °C to 150 °C.

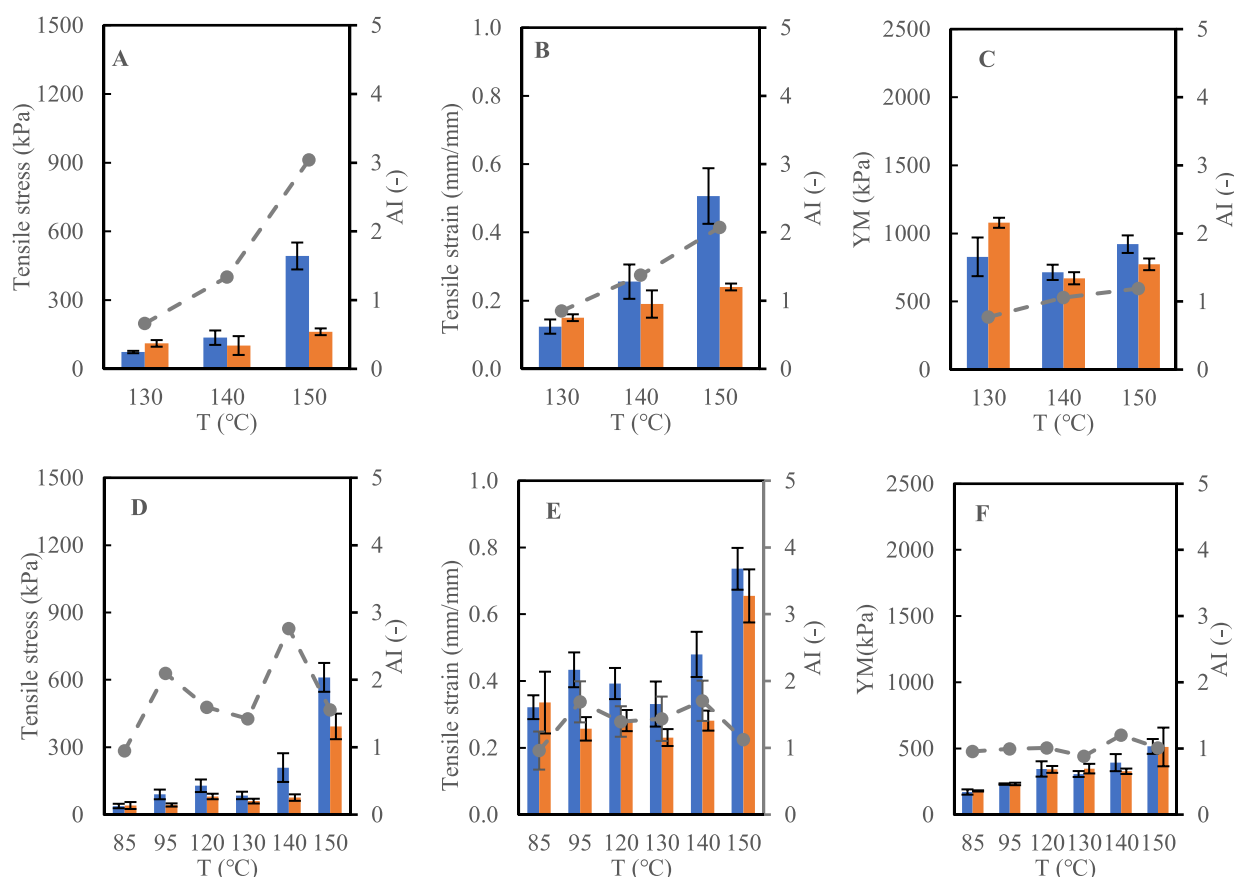| T	95 °C	120 °C	130 °C	140 °C	150 °C
RPC-only	NA				
RPC-WG					

Fig. 1. Tensile stress (A), tensile strain (B) and YM (C) of the sheared 40 wt% RPC sample at 130, 140 and 150 °C. Tensile stress, tensile strain and YM of the 40 wt% RPC-WG at 85, 95, 120, 130, 140 and 150 °C are shown in (D), (E) and (F). Blue bars indicate the parallel direction, orange bars indicate the perpendicular direction and the dotted grey line indicates the anisotropic index (AI). The statistical analysis is showed in the appendix Table S1. (For interpretation of the references to colour in this figure legend, the reader is referred to the web version of this article.)

Table 4
Macrostructure of SPC (40 wt%) and SPC-WG (20–20 wt%) at 95 °C, 120 °C and 140 °C.

T	95 °C	120 °C	130 °C	140 °C	150 °C
SPC-only					
SPC-WG					

plastic beaker. RPC and SPC were added to the beaker and mixed using a flat spoon, which was covered with a parafilm to prevent water evaporation. WG, if used in mixtures, was added after 30 min hydration, mixed thoroughly with a flat spoon and immediately transferred to a shear cell for further processing.

2.2.2. Structure formation

A high-temperature conical shear cell (HTSC) (Wageningen University, Wageningen, the Netherlands) was used for the structuring experiments. The HTSC was designed in house and has been described previously. It is a cone-cone device with a rotating bottom cone to produce a defined simple shear flow (Grabowska et al., 2016b). Heating and cooling was done using an external oil bath. The protein mixtures, which were hydrated for 30 min before shearing, were transferred to the preheated HTSC and then sheared for 15 min at 30 rpm at a set

temperature. Different temperatures were tested in this study form 85 °C to 150 °C. The shearing was stopped and the shear cell was cooled down to 25 °C in 15 min to allow removal of the pancake-shaped sample. The sample was stored in a plastic bag. All tests were done in duplicate.

2.3. Analysis

2.3.1. Macrostructure

The morphologies of sheared and heated products of RPC, SPC-only, and the mixtures of RPC-WG, SPC-WG were analysed by manually deforming the samples in a direction parallel to the shear flow and then the structure formed was inspected visually.

2.3.2. Colour measurement

The colour of the sheared samples from RPC-only and RPC-WG
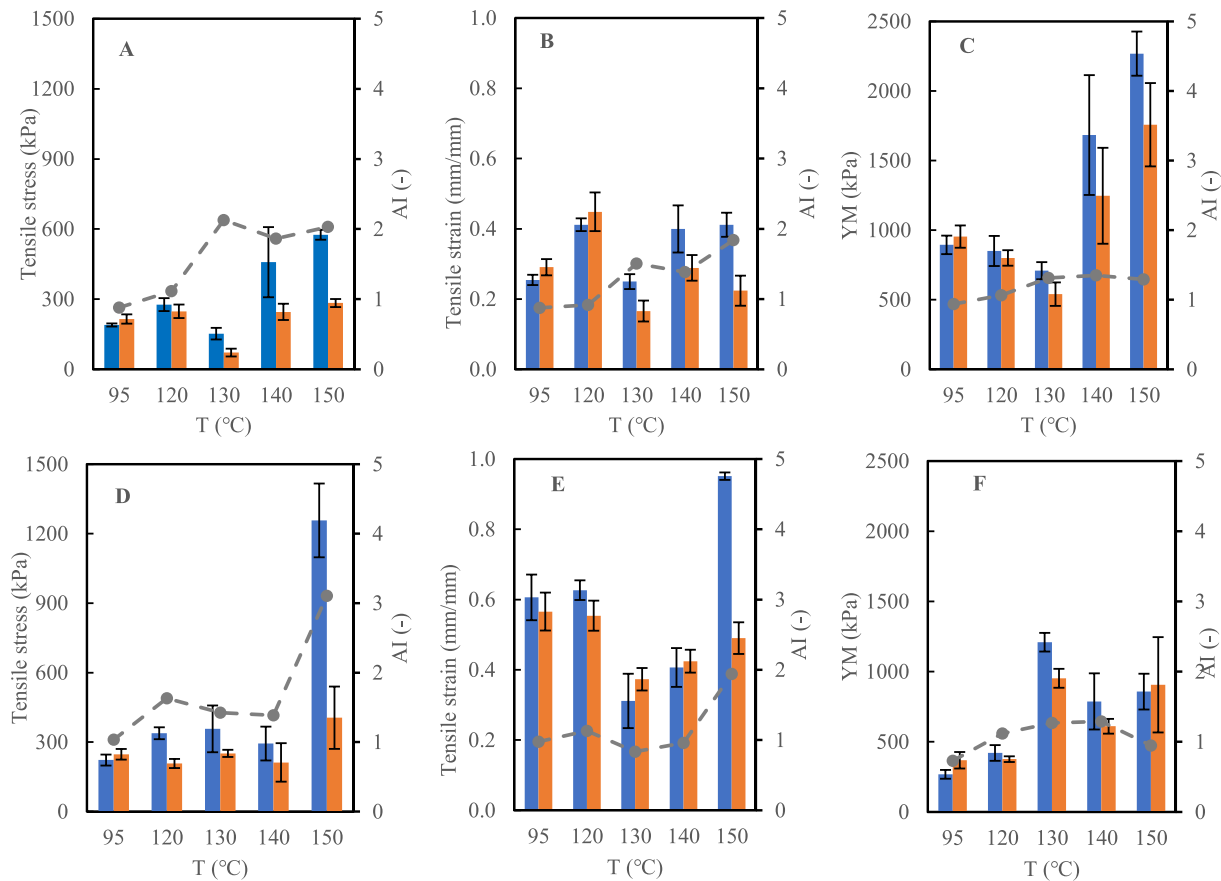
Fig. 2. Tensile stress (A), tensile strain (B) and YM (C) of the 40 wt% SPC. Tensile stress, tensile strain and YM of 40 wt% SPC-WG of 20:20 are shown in (D), (E) and (F). Temperatures of 95, 120 and 140 °C were tested. Blue bars indicate the parallel direction, orange bars indicate the perpendicular direction and the dotted grey line indicates the anisotropic index (AI). The statistical analysis is showed in the appendix Table S1. (For interpretation of the references to colour in this figure legend, the reader is referred to the web version of this article.)

Table 5
Macrostructure of RPC-WG and SPC-WG with ratios of 40–0, 32–8, 26–14, 20–20, 14–26, 8–32, 0–40 wt% at 140 °C.

RPC-WG	40–0 wt%	32–8 wt%	26–14 wt%	20–20 wt%
Macrostructure				
RPC-WG Macrostructure	14–26 wt%	8–32 wt%	0–40 wt%	
SPC-WG Macrostructure	40–0 wt%	32–8 wt%	26–14 wt%	20–20 wt%
SPC-WG Macrostructure	14–26 wt%	8–32 wt%	0–40 wt%	

mixtures were determined using a colorimeter (Chroma Meter CR-400, Konica Minolta, Country). The colour intensity was indicated as L* (perceptual lightness), a* (−a* = green and + a* = red) and b* (−b* = blue and + b* = yellow).

2.3.3. Tensile strength analysis

The mechanical properties of the sheared samples were measured using a texture analyser (Stable Micro System, Godalming, UK). Tensile stress, tensile strain and Young's modulus (YM) were measured by uniaxial tensile tests, which were performed at room temperature with a

Fig. 3. Tensile stress, tensile strain and YM for RPC-WG and SPC-WG at ratios of 40–0, 32–8, 26–14, 20–20, 14–26, 8–32 and 0–40 wt% are shown. Shearing conditions of 140 °C, 30 rpm and 15 min were tested. Blue bars indicate the parallel direction, orange bars indicate the perpendicular direction and the dotted grey line indicates the anisotropic index (AI). The statistical analysis is showed in the appendix Table S1. (For interpretation of the references to colour in this figure legend, the reader is referred to the web version of this article.)

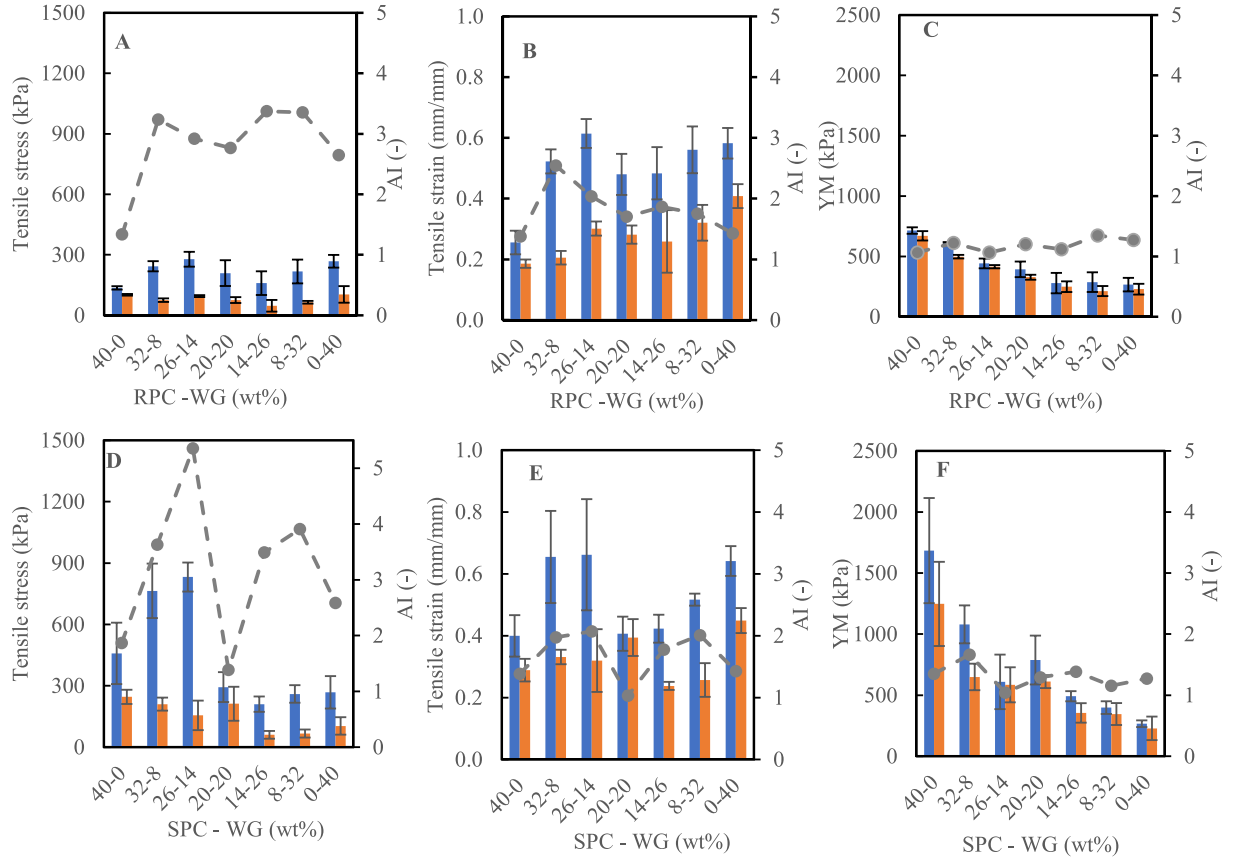constant deformation speed of 1 mm/s. Three tensile bars were cut from the samples using a dog-bone-shaped cutter in the parallel and perpendicular directions along the shearing direction. The width and thickness of the tensile bars were then measured using a digital calliper (Mitutoyo, Kawasaki, Japan) to calculate the initial cross-sectional area. The edges of the tensile bars were fixed into tensile grips, resulting in an initial length of 15.5 mm (L_0) for the sample. The force needed to break the sample (t) was recorded by the Exponent software (Stable Micro System). The true stress (σ) and true strain (ε) were calculated based on the assumption that the volume of the tensile bar did not change during elongation (Choung & Cho, 2008; Raheem, 2014).

$$\sigma = \frac{F(t)}{A_0} \times \frac{L(t)}{L_0} \ [\text{Pa}] \tag{3}$$

$$\varepsilon = ln\frac{L(t)}{L_0} \ [\text{mm/mm}] \tag{4}$$

where L_0 is the initial length of the sample and $L(t)$ is the length of the sample at fracture time t. A_0 is the initial cross-sectional area. YM was calculated from the slope of the tensile stress-strain curve with the tensile strain between 0.5 and 1.5. The anisotropic index (AI) was calculated as the quotient of the parallel value and the perpendicular value:

$$AI_\sigma = \frac{\sigma_{\text{par}}}{\sigma_{\text{per}}} \ [-] \tag{5}$$

$$AI_\varepsilon = \frac{\varepsilon_{\text{par}}}{\varepsilon_{\text{per}}} \ [-] \tag{6}$$

$$AI_{\text{YM}} = \frac{\text{YM}_{\text{par}}}{\text{YM}_{\text{per}}} \ [-] \tag{7}$$

2.3.4. Microstructure

A confocal laser scanning microscope (type 510; Zeiss, Oberkochen, Germany) was used to visualize the structured samples on a microscopic scale. RPC-WG and SPC-WG mixtures were frozen before cutting the samples along the shear flow direction into rectangular shapes with dimension of approximately 3 × 5 × 10 mm. The samples were frozen quickly using liquid nitrogen. A cryomicrotome (Micron CR50-H, Adamas Instruments, Rhenen, the Netherlands) was used at −20 °C to slice the sample into 40-μm-thick specimens. The specimens were then stained with a mixed solution of Rhodamine B 0.002 wt% and Calcofluor White 0.01 wt% at a 1:1 ratio, after which they were covered with a glass and stored in dark for 1 h before analysis.

Excitation light in CLSM was provided by two lasers: a HeNe laser at 543 nm for Rhodamine B, and a blue/violet diode laser at 405 nm for Calcofluor White. A 10× EC Plan-Neofluar/0.5 objective lens was used to take the images. The blue edition of the ZEN software (Carl Zeiss Microscopy, Jena, Germany) was used to analyse the images.

2.3.5. Morphology

Scanning Electron Microscope (SEM) (JEOL JCM-7000, the Netherlands) was used to observe the morphology of the RPC, SPC and WG dry powders. The dry samples were added on the double-side adhesive conductive carbon tabs and the samples were sputter-coated with gold. Compressed air was used to distribute the sample evenly on the surface of carbon tabs. The accelerating voltage was 10 kV. The SEM
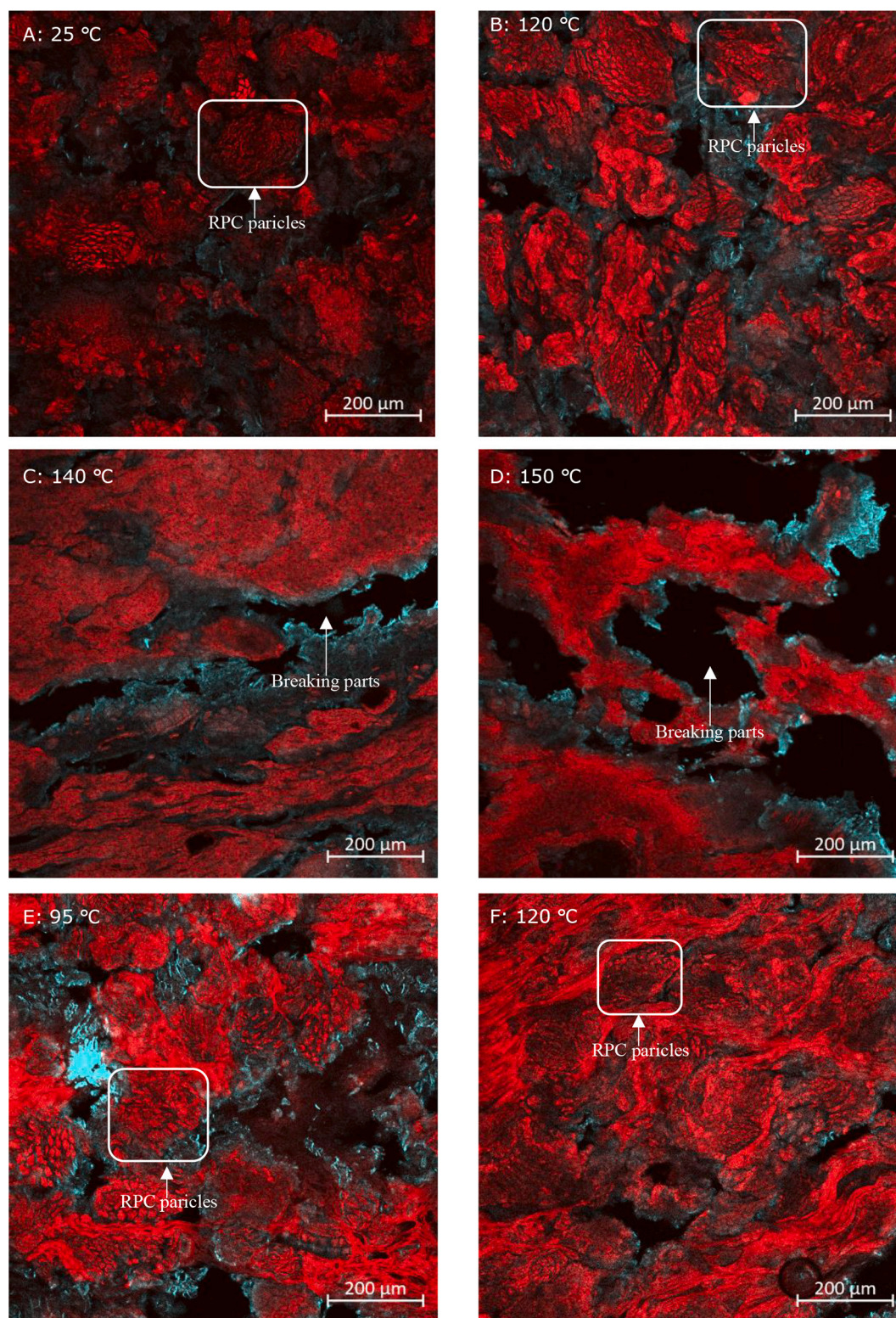
Fig. 4. Microstructure of the sheared products from RPC-only was obtained at shear temperatures of (A) 25 °C, (B) 120 °C, (C) 140 °C and (D) 150 °C by CLSM under the fluorescence channel. The sheared product from RPC-WG (20–20 wt%) at 95 °C and 120 °C is shown in (E) and (F). The products were sheared at 30 rpm by 15 min. Scale bars, 200 μm; each image was selected from three images.

pictures were taken at a scale of 50 μm.

2.3.6. X-ray microtomography

Inclusion of air in the fibrous products was analysed non-invasively and non-destructively using XRT (GE Phoenix v|tome|x m; General

Electric, Wunstorf, Germany). A 240 kV micro focus tube with tungsten target was used with a voltage of 80 kV and a current of 90 μA. The images were recorded by a detector (GE DXR detector array with 2024 × 2024 pixels and pixel size 200 μm) located 815 mm from the X-ray source. Fragments 4 × 5 × 20 mm were cut from the sheared
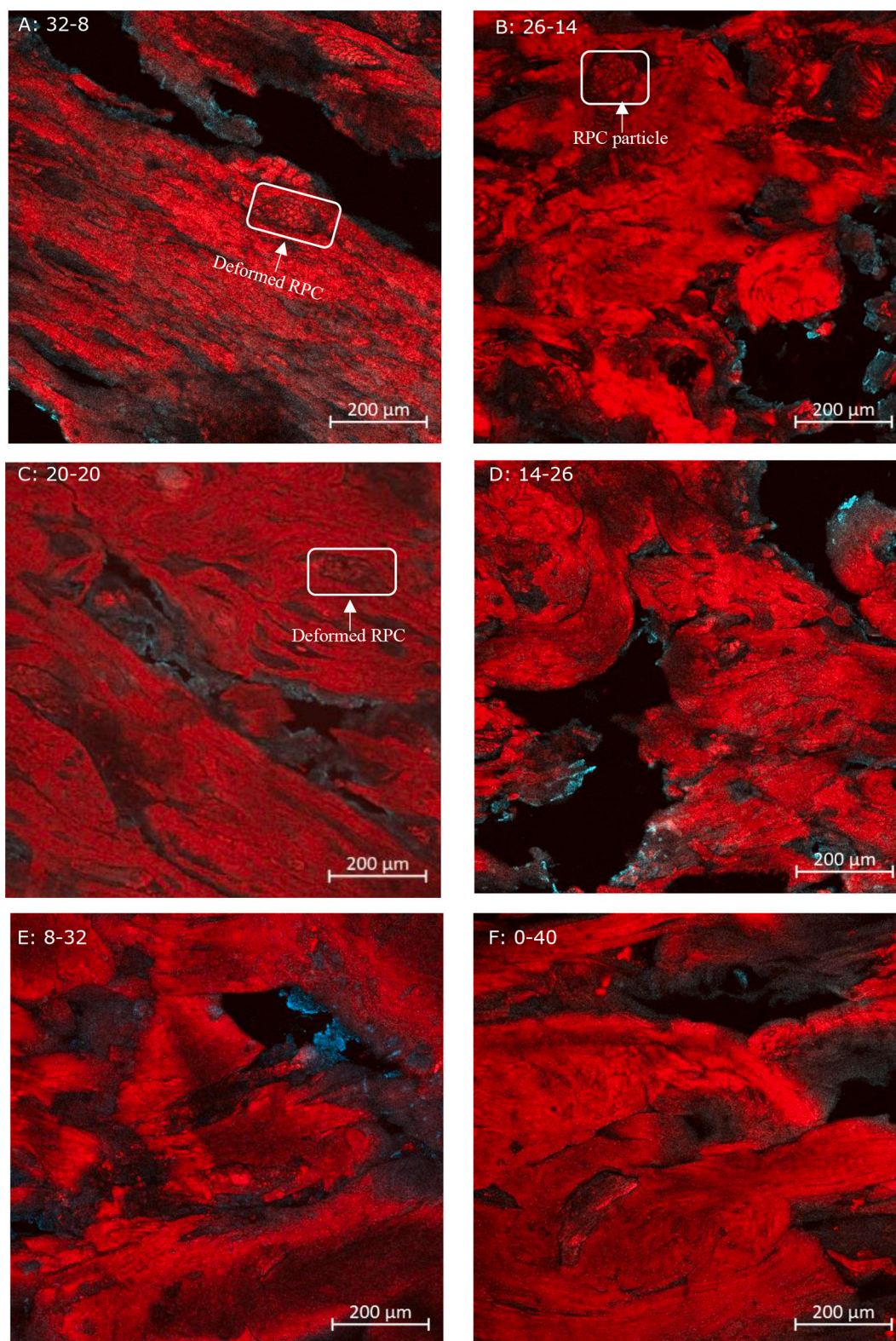
Fig. 5. Microstructure of the sheared products from RPC-WG at ratios of 32–8, 26–14, 20–20, 14–26, 8–32 and 0–40 wt% under process conditions of 140 °C, 30 rpm and 15 min by CLSM under the fluorescence channel. Scale bars, 200 μm; each image was selected from three images.

samples. The fragments were placed into an Eppendorf tube to avoid moisture loss and positioned 28.55 mm from the X-ray source, resulting in a spatial resolution of 7 μm. Full scans of 1500 projections were taken by placing the sample on a rotary stage over 360° with steps of 0.24°. The projections obtained were reconstructed into a single 3D structure using the GE reconstruction software (GE, Wunstorf, Germany), with the first projection skipped. Reconstructed images of the samples were analysed using Avizo imaging software version 9.2.2. Two reconstructed images were used to calculate the porosity of the samples.
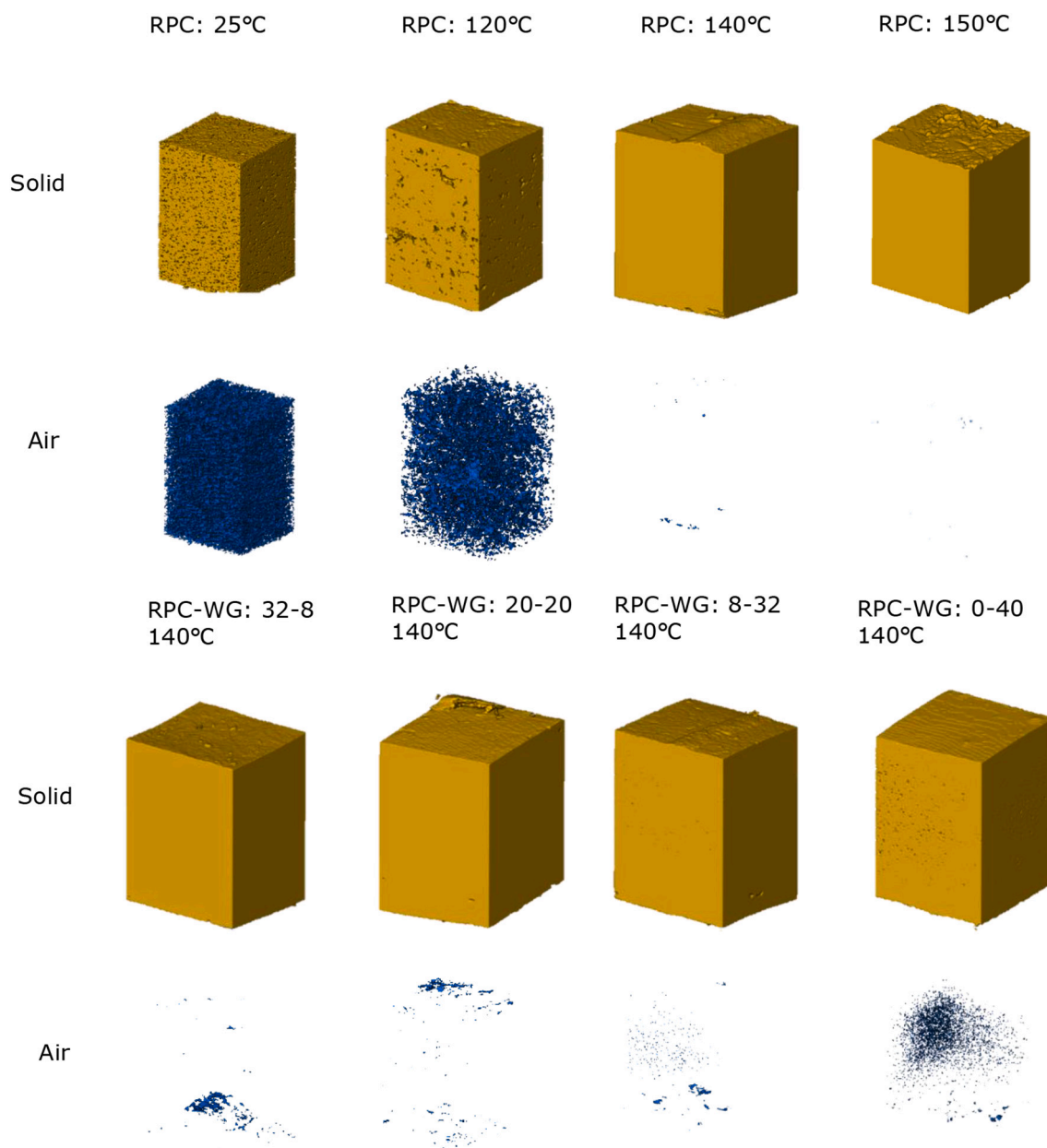
Fig. 6. X-ray microtomography images of a reconstructed trimetric image of the solid (yellow) sheared 40 wt% RPC product at 25, 120, 140 and 150 °C and RPC-WG product with ratios of 40–0, 32–8, 20–20, 8–32 and 0–40 wt% at 140 °C and the corresponding reconstructed trimeric image of the air in blue. (For interpretation of the references to colour in this figure legend, the reader is referred to the web version of this article.)

2.3.7. Statistical analysis

The statistics in this paper were analysed using SPSS software, version 25.0 (IBM, Armonk, NY, USA). A univariate general linear model with the least significant difference (LSD) test was carried out to investigate the significant differences with respect to Figs. 1–3. Differences were considered significant when $P < 0.05$, which are shown in the appendix Table S1. The same test was applied to the colour measurement and the differences are shown as the small letters in Fig. 9.

3. Results

3.1. Effect of temperature effect on the structuring properties

3.1.1. RPC-only and SPC-only

RPC-only dispersions with 40 wt% were sheared at 120 °C, 130 °C, 140 °C and 150 °C in the shear cell. The resulting structures are shown in Table 3. A fibrous structure was obtained after processing at 140 °C or 150 °C; the latter resulted in a more pronounced fibrous material. A crumbled gel-like structure was obtained when RPC was sheared at lower temperatures of 120 °C or 130 °C. The mechanical properties of the sheared and heated products were measured using a texture analyser and the results are shown in Fig. 1. For RPC-only, tensile stress and strain values in the parallel direction increased with higher temperature, whereas the value in the perpendicular direction was similar for all temperatures. The AI value was >1 after processing at 140 °C, which corresponds to the mechanical anisotropy. The sample produced at 120 °C was too brittle to allow good measurements. Shearing at 150 °C led to more anisotropy, up to an AI value of 3. Results showed that YM was independent of temperature in both directions, and thus the stiffness of the product was similar after processing at different temperatures.

To place the results with RPC in a broader context, we compared its structuring capacity with SPC. The macrostructure of SPC-only product
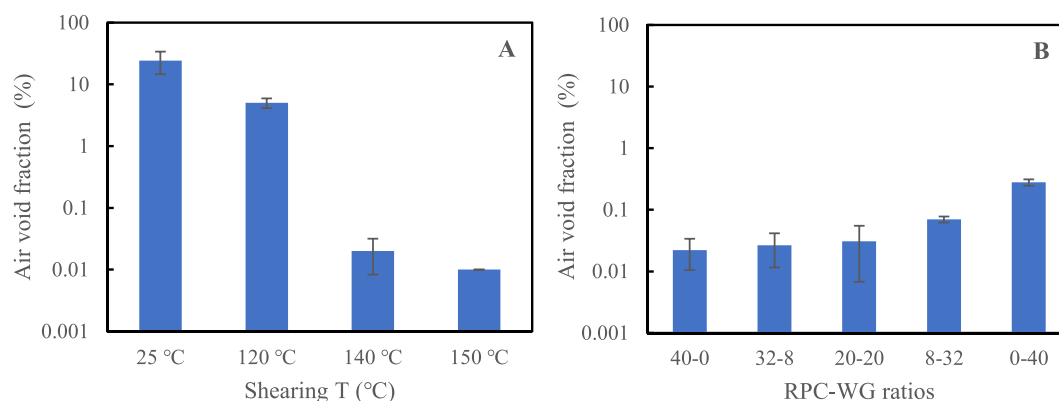
Fig. 7. Air void fraction of sheared RPC product at 25 °C, 120 °C, 140 °C and 150 °C (A) and sheared RPC-WG products with RPC ratios of 40–0, 32–8, 20–20, 8–32 and 0–40 wt% (B).

is shown in Table 4. For the SPC-only sheared product, a crumble structure was observed below 120 °C. Thin fibres and layers were found when SPC-only was sheared at 140 °C. The mechanical properties of the SPC-only products are shown in Fig. 2(A–C). The value for the tensile stress in the parallel direction increased with higher process temperature, with an exception for the product processed at 130 °C. The tensile stress in the perpendicular direction appeared to be independent of temperature, again except at 130 °C. As a result, the AI value increased when processing at a higher temperature. With respect to the tensile strain, the lowest value was observed at 130 °C. Although the values in the parallel and perpendicular direction fluctuated at different temperatures, the AI value increased from 1 to 2 in the temperature range studied. The YM decreased in both directions when a higher temperature was applied, resulting in similar AI values.

3.1.2. RPC-WG and SPC-WG mixtures

The 20–20 wt% RPC-WG mixture led to lighter coloured fibrous products when processed at 130 °C and 140 °C. A gel-like structure with tiny fibres was formed at 150 °C for RPC-WG, whereas a gel-like and crumble structure was generated at 95 °C and 120 °C. Mostly, the tensile stress in the parallel direction increased with temperature, except for a slight decrease when processed at 130 °C. Although the trend for the perpendicular direction was less obvious, the highest value was obtained at 150 °C. The AI value remained between 1 and 2 at most temperatures, which suggests limited mechanical anisotropy. The highest AI value of 2.8 was obtained for tensile stress in the parallel direction at 140 °C. The YM of RPC-WG products showed a slight increase with increasing temperature for both directions, but the values were much lower compared with the RPC-only product. The AI value of the RPC-WG product sheared at 150 °C was nearly 1, which is in line with the gel structure observed in Table 3. The structures of sheared products with respect to the 20–20 wt % SPC-WG mixture processed at 95 °C, 120 °C, 130 °C and 140 °C are shown in Table 4. The 20–20 wt% SPC-WG product showed a crumble gel structure below 130 °C similar to the RPC-WG product. A gel structure with layers was obtained after processing at 140 °C and 150 °C.

The mechanical properties of the SPC-WG products are shown in Fig. 2D–F. The highest tensile stress was found at 150 °C. This led to the highest AI value of 3, which was similar to the AI value for the RPC-only product at 150 °C. However, no fibrous structure was observed at 150 °C despite the high AI value. This might be because the fibrous structure was too small to be visible by eye, and the current methods in fibrous structure quantification is still limited (Floor K.G. Schreuders, Schlangen, Kyriakopoulou, Boom, & van der Goot, 2021). From the observation, the product structure could be characterized best as a gel with layers (Table 4). At lower processing temperatures, lower tensile stress values were found for both directions; they were similar to the value in the perpendicular direction leading to an AI value of ~1. The lowest tensile strain value was obtained when processing at 130 °C. Due to a

decrease in tensile strain for both directions at 130 °C and 140 °C, a similar AI value of 1 was found for both products. An increase in YM was found at 130 °C, and the AI value of YM was slightly increased from 95 °C to 140 °C.

Despite the differences in the mechanical properties, the structures observed for the SPC-only and SPC-WG products were hardly dependent on the temperature at 40 wt%. In the case of RPC-only and RPC-WG products, a processing temperature of 140 °C was sufficient to obtain fibrous products. Therefore, 140 °C was applied in further investigations of the fibrous structure at different RPC and WG ratios.

3.2. Effect of composition on the structuring properties

This section describes the effect of adding different amounts of WG to the RPC and SPC on the structure of the products (Table 5). All RPC-WG products showed a fibrous structure. The RPC-WG mixtures were a light grey colour, which became more brown when the product contained more RPC. The tensile stress values of the RPC-WG mixtures (Fig. 3) were between 100 and 300 kPa for the parallel direction and ranged from 50 to 100 kPa for the perpendicular direction. On average, AI values of ~3 were obtained, which were higher than the average AI value of 1.3 for the RPC-only sample. The large standard deviation of the tensile stress in the parallel direction was probably caused by the heterogeneity of the fibrous material at the length scale of the sample. Fibres were clearly visible in that size range. When overviewing all the mechanical data of RPC-WG, AI value was approximately 3 for all the ratios. The fibrous structure formed was different at low WG ratios for 32–8 and 26–14 wt% compared to higher WG ratios between 20 and 20 and 8–32 wt%. An increase in WG led to more pronounced fibrous products with tiny fibres and even more than the WG-only product.

In the case of SPC-WG products, gel-like structures were observed with 32–8 wt% (Table 5), which is similar to SPC-only. Gel-like structures with layers were formed with the product containing SPI-WG ratios of 26–14 and 20–20 wt%. The fibrous structure became more pronounced when the product contained more WG. The tensile stress for the parallel direction increased from products containing SPC-WG with ratios of 40–0 to 26–14 wt%, whereas the value decreased in the perpendicular direction leading to a highest AI value of 5 for the product with the ratio 26–14 wt%. This result indicated that the addition of WG to SPC enhanced the anisotropy of tensile stress and strain; the 20–20 wt % product was the exception.

The YM decreased when the WG content increased in the RPC-WG and SPC-WG products and this effect was also found to be higher with the SPC-WG product. The AI value for the YM was close to 1 for almost all products. Thus, the addition of WG above a certain ratio can improve the fibrous structure formation for the SPC-WG and RPC-WG products.
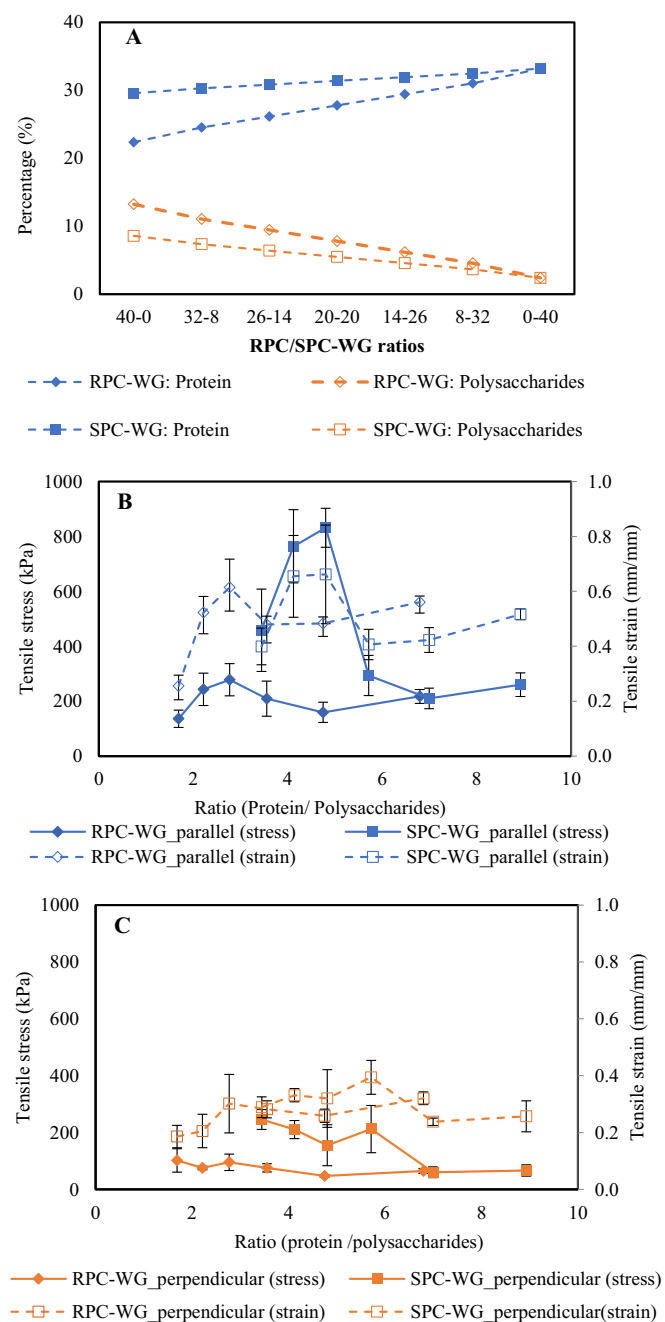
Fig. 8. The composition (A) of protein and polysaccharides of the RPC-WG mixtures and SPC-WG mixtures. The tensile stress (kPa) and tensile strain (mm/mm) of RPC-WG and SPC-WG mixtures at parallel direction (B) and perpendicular direction (C) as a function of the protein and polysaccharides ratio.

3.3. Microstructure

CLSM was used to examine the microstructure and the distribution of protein and polysaccharides in the sheared RPC and RPC-WG products. The results obtained with the fluorescence channel are shown in Figs. 4 and 5.

For the sheared RPC-only products, intact RPC particles were observed at room temperature and after processing at 120 °C (Fig. 4). These particles were found to be similar as observed by SEM pictures in the appendix (Fig. S2), with the particle size of approximately 200 μm (Jia, Rodriguez-Alonso, Bianeis, Keppler, & van der Goot, 2021). The

RPC particles are consisted of proteins (stained red) surrounded by polysaccharides (represented by the blue colour). The polysaccharide phase became better visible at 120 °C onwards. This might be due to the finely dispersed unheated RPC particles became aggregated by heating and hearing at higher temperatures. The intact RPC particles disappeared at 140 °C, forming a more continuous protein phase and dispersed polysaccharide phase. The structure was broken apart during sample preparation and the breaking part were found within the polysaccharide phase in Fig. 4C and D. In the case of RPC-WG 20–20 wt%, individual RPC particles were still observed at 95 °C and 120 °C (Fig. 4E and F); the WG already formed a connected phase between the individual RPC particles, thus forming another phase.

The RPC particles disappeared for the 20–20 wt% product when the material was processed at higher temperatures of 140 °C, although a few deformed RPC particles were still visible (Fig. 5C). The microstructures of RPC-WG with other ratios processed at 140 °C are also shown in Fig. 5. Similar to the 20–20 wt% RPC-WG product, deformed RPC particles were visible in the 32–8 wt% RPC-WG product. These deformed RPC particles consisted of protein and fibre and were dispersed in a continuous phase. However, the proteins from RPC and WG were hardly distinguishable for all the mixing ratios tested at 140 °C, which indicates that the protein from RPC and WG was mixed at a much smaller length scale than visible with CLSM (i.e. 200 μm).

3.4. Incorporation of air

The reconstructed 3D X-ray tomography image of air in Fig. 6 showed air inclusion (void fraction) in RPC product when sheared at 25 °C. The void fraction became smaller when the products were sheared at a higher temperature. Hardly any air remained after shearing the products at 140 °C and 150 °C. The overall void fractions are shown in Fig. 7A. The void fraction decreased from 24 vol% for the product sheared at 25 °C to 5 vol% when the products were sheared at 120 °C. Almost all air had escaped when the product was processed at 140 °C, and an even lower void fraction of 0.01 vol% was measured after processing at 150 °C. These results could be explained by considering that the hydrated RPC particles were not fully melted at lower temperature, thus spaces remained available for air between the particles. The void fractions obtained with the sheared RPC-WG product were all <0.3 vol% at 140 °C, whereas slightly more air was found with the RPC-WG mixture of 8–32 wt% and 0–40 wt% in Fig. 7B. Therefore, it is suggested that the air void fraction of the sheared product is more dependent on the processing temperature than the RPC-WG ratios at 140 °C.

4. Discussion

Previous research revealed the importance of naturally existing immiscible phases of protein and polysaccharides for fibrous structure formation by SPC-only or SPI/pea protein isolate-WG mixtures in the shear cell (Grabowska et al., 2016a; Schreuders et al., 2019). Here, we aimed to demonstrate that fibrous materials can also be obtained with RPC-only, similar to SPC-only, by using the remaining polysaccharides in the material as a second phase. We also aimed to test the effect of adding WG as an additional phase to the RPC on the structuring capacity.

Fibrous material in 40 wt% RPC-only was achieved at 140 °C and 150 °C. In contrast, the SPC-only sheared product of 40 wt% at these temperatures was characterized as a layered gel with some tiny fibres. This result was similar to previous results for a 40 wt% SPC-only sheared product; a fibrous structure was reported when the dry mass content was increased to 45 wt% with SPC-only (Grabowska et al., 2016b). However, we found the tensile stress at 140 °C to be higher than reported earlier, which we attributed to different batches of SPC. Grabowska et al. (2016b) used the break-up and alignment of the polysaccharide phase as an explanation for the fibrous structure formation for the sheared SPC-only product at 140 °C. Here, it is hypothesized that melting of RPC
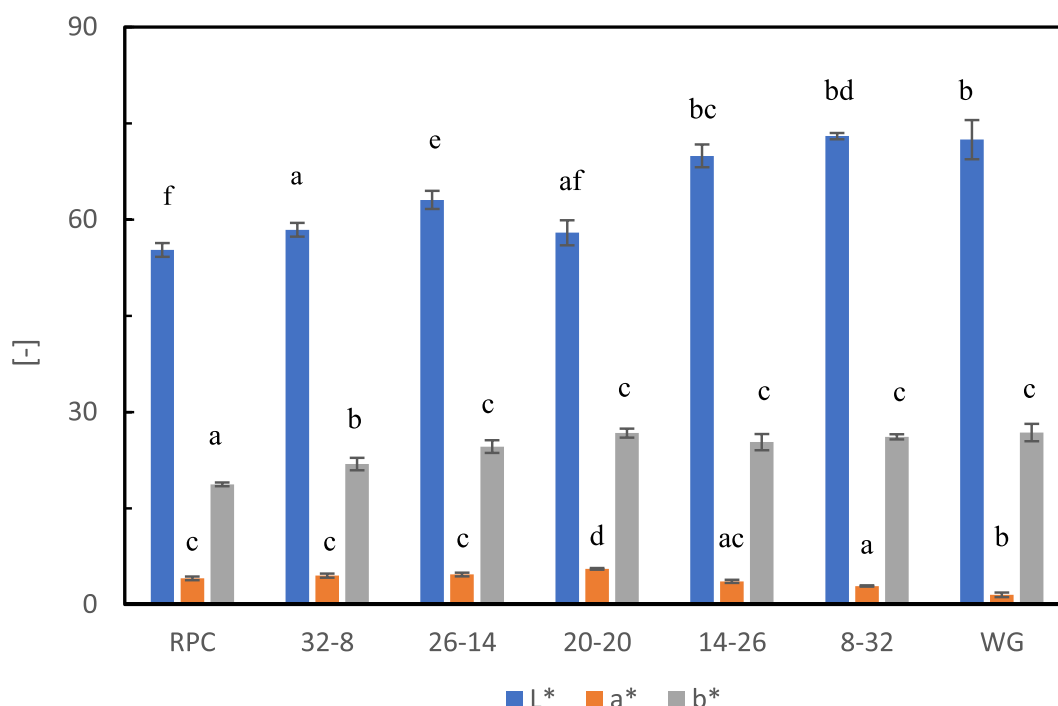
Fig. 9. Colour intensity of the sheared RPC-only, RPC-WG mixtures at different ratios and WG-only products, indicated as L* (perceptual lightness), a* (−a* = green and + a* = red) and b* (−b* = blue and + b* = yellow). The statistics were analysed with respect to L*, a* and b* individually and showed as the small letters. (For interpretation of the references to colour in this figure legend, the reader is referred to the web version of this article.)

particles (consisting of protein and polysaccharides) happened at 140 °C, which explains the need for a high temperature (Fig. 4). Without this melting, RPC still behaves as a sand-like material that hardly takes up water during hydration, as we observed when mixing RPC and water at room temperature. Melting of RPC at 140 °C makes it possible for the polysaccharides to be more easily aligned along the shearing direction and thus act as a dispersed phase to the proteins.

Similarly, RPC particles melting at 140 °C released proteins from the particles, and the proteins were mixed with WG in subsequent shearing in the RPC-WG mixtures. This can explain the continuous protein phase with no clear phase separation between the protein from WG and RPC after shearing and heating at 140 °C (Section 3.3). Furthermore, with respect to the 20–20 wt% RPC-WG and SPC-WG mixtures, a temperature of 130 °C was sufficient to create fibrous structures in both cases (Tables 3 and 4), but the mechanical properties were found to be relatively low at that temperature (Figs. 1 and 2). In the above discussion, it is hypothesized that the melting of RPC particles at 140 °C and subsequent availability of proteins is a prerequisite for fibre formation in RPC-only. Similar to that observation, the RPC particles in the RPC-WG mixture are not melted sufficiently at 130 °C, whereas WG already acts as a continuous phase and thus induces fibre formation at lower temperatures than observed for RPC-only, but the dispersed phase will be weak because of lack of melting. Therefore, the effect of adding WG to RPC might play an important role to reduce the temperature required for fibre formation. Schreuders et al. (2019) reported fibrous structure formation for PPI-WG (20–20% wt) at 120 °C and SPI-WG (20–20 wt%) at 140 °C, and the lowest mechanical properties were found at 130 °C. In that paper, WG was introduced as a second phase. A similar air inclusion effect as reported for PPI and SPI-WG mixtures was also observed for the RPC-WG sheared products at different shearing temperatures (Section 3.4). The low air porosity found at 140 °C for RPC-only and RPC-WG mixtures also suggests the melting of RPC particles and the formation of a compact structure. However, further investigations would be needed to understand the two-phase system when WG is added to the RPC-WG mixtures at different temperatures.

A dry mass of 40 wt% was needed for the fibrous structure formation for RPC-only, results showed in the appendix Fig. S1, which is lower compared with 45 wt% for SPC-only (Grabowska et al., 2016a). A comparison between RPC and SPC reveals that RPC has a lower protein content (22.4 vs 29.6 wt%) and higher polysaccharide content (13.2 vs 8.6 wt%) than SPC. In the case of the RPC-WG and SPC-WG mixtures, less WG was required for fibrous structure formation with RPC than for SPC. This yielded a wider range of ratios required for fibrous structure formation with respect to the RPC-WG product (32–8 to 8–32 wt%) compared with the SPC-WG product (26–14 and 8–32 wt%) (Fig. 8A and Table 5). The composition of the mixtures with respect to protein and polysaccharides might affect the fibrous structure formation. The addition of WG to the concentrates increased the overall protein content and decreased the polysaccharide content. Thus, we plotted the tensile properties of all the tested materials at 140 °C against protein/polysaccharides ratios (Fig. 8B and C). The tensile properties were enhanced with increasing protein ratio (below 6 for SPC-WG 20–20 wt%) and the minimum AI value was found at 20-20 wt%, but no fibrous structure was found in this region. This result suggested a change of the system from soy protein continuous phase into the WG continuous phase, and the change is hypothesized to be with the ratio of 20–20 wt%. Cornet et al. (2021) also reported that structuring the protein mixtures with respect to the SPI-WG and fababean isolate-WG in Shear Cell resulted in fibrous structures at gluten contents ≥0.5 wt/wt and the effect of gluten on swelling and fibre formation is universal for the tested proteins. A fibrous structure formed with ratios ranging between 2 and 7 for RPC-WG and 7–9 for SPC-WG, which suggests that a higher protein/polysaccharides ratio is necessary for fibrous structure formation with SPC-WG than for RPC-WG. The ratio of protein/polysaccharide might be one of the factors to explain the effect of the composition on fibrous structure formation. Besides protein/polysaccharides ratio, the other factors might also play a role in the structuring properties, such as amino acid profile and rheological characterization upon melting. Cysteine and methionine are the sulphur containing amino acid, which is important for the cross-linking properties by forming disulphide bonding upon

heating (Berghout, Boom, & van der Goot, 2015). Furthermore, not only the amount of disulphide bonds in the protein plays a role, but also the accessibility of disulphide and free thiol groups is important for network formation (Cornet et al., 2020). Further investigation on these factors is still required to explain why a certain ratio is necessary.

The composition and the ratio of the concentrate are not only influences the mechanical properties of the fibrous structure formed but also the colour of the final product. The product became lighter when more WG was added in the RPC-WG mixtures (Table 5). The colour of the sheared sample was measured by the colorimeter, indicating as L* (perceptual lightness), a* (−a* = green and + a* = red) and b* (−b* = blue and + b* = yellow). Results in Fig. 9 showed that L* and b* was significantly increased by adding of the WG into RPC till the RPC-WG ratio of 26–14, while the intensity of a* was similar between the ratio of 40–0 and 26–14, and significantly decreased by further adding of WG. The change in the colour is not necessarily related to change in the dominant continuous protein phase because both proteins from RPC and WG were mixed thoroughly which is hard to distinguish on the product scale (Section 3.2). It is most likely that the addition of lighter coloured WG diluted the already darker coloured RPC content. In addition, oxidized tannins in RPC form darkly coloured polymers during processing at high temperatures. In the presence of WG, however, such oxidized tannins could react with available thiol groups from WG instead of polymerizing, which would reportedly form uncoloured complexes (Keppler, Schwarz, & van der Goot, 2020; Ozdal, Capanoglu, & Altay, 2013).

5. Conclusion

This study reveals the potential of RPC as a novel ingredient for application in meat analogues. RPC could be used to make fibrous products even without the presence of WG. In addition, RPC formed more pronounced fibres compared with SPC under the same conditions. Also in combination with WG, we noticed that RPC offers more possibilities to create a wide range of fibrous products compared with SPC at 140 °C. This is due to the fact that complete melting of RPC particles only occurred at a processing temperature of 140 °C or above. The addition of WG into RPC at 140 °C showed two effects: improved anisotropic structure with increased AI value on tensile stress for all ratios; lighter colour of the sheared RPC-WG product than the RPC-only product. The structure formation observed in the RPC-/SPC-only product was explained by the presence of polysaccharides in those ingredients, although the mechanism of the exact structure formation process is not yet fully understood.

Supplementary data to this article can be found online at https://doi.org/10.1016/j.ifset.2021.102758.

Declaration of Competing Interest

None.

Acknowledgements

References

Asgar, M. A., Fazilah, A., Huda, N., Bhat, R., & Karim, A. A. (2010). Nonmeat protein alternatives as meat extenders and meat analogs. *Comprehensive Reviews in Food Science and Food Safety, 9*(5), 513–529. https://doi.org/10.1111/j.1541-4337.2010.00124.x

Banovic, M., & Sveinsdóttir, K. (2021). Importance of being analogue: Female attitudes towards meat analogue containing rapeseed protein. *Food Control, 123*(October 2020). https://doi.org/10.1016/j.foodcont.2020.107833

Berghout, J. A. M., Boom, R. M., & van der Goot, A. J. (2015). Understanding the differences in gelling properties between lupin protein isolate and soy protein isolate. *Food Hydrocolloids, 43*, 465–472. https://doi.org/10.1016/j.foodhyd.2014.07.003

Choung, J. M., & Cho, S. R. (2008). Study on true stress correction from tensile tests. *Journal of Mechanical Science and Technology, 22*(6), 1039–1051. https://doi.org/10.1007/s12206-008-0302-3

Cornet, S. H. V., Bühler, J. M., Goncalves, R., Bruins, M. E., van der Sman, R. G. M., & van der Goot, A. J. (2021). Apparent universality of leguminous proteins in swelling and fibre formation when mixed with gluten. *Food Hydrocolloids*, 106788. https://doi.org/10.1016/j.foodhyd.2021.106788

Cornet, S. H. V., Snel, S. J. E., Schreuders, F. K. G., van der Sman, R. G. M., Beyrer, M., & van der Goot, A. J. (2020). Thermo-mechanical processing of plant proteins using shear cell and high-moisture extrusion cooking. *Critical Reviews in Food Science and Nutrition*, 1–18. https://doi.org/10.1080/10408398.2020.1864618

Dekkers, B. L., Nikiforidis, C. V., & van der Goot, A. J. (2016). Shear-induced fibrous structure formation from a pectin/SPI blend. *Innovative Food Science and Emerging Technologies, 36*, 193–200. https://doi.org/10.1016/j.ifset.2016.07.003

Draganovic, V., Boom, R. M., Jonkers, J., & Van Der Goot, A. J. (2014). Lupine and rapeseed protein concentrate in fish feed: A comparative assessment of the techno-functional properties using a shear cell device and an extruder. *Journal of Food Engineering, 126*, 178–189. https://doi.org/10.1016/j.jfoodeng.2013.11.013

Grabowska, K. J., Tekidou, S., Boom, R. M., & van der Goot, A. J. (2014a). Shear structuring as a new method to make anisotropic structures from soy–gluten blends. *Food Research International, 64*, 743–751. https://doi.org/10.1016/j.foodres.2014.08.010

Grabowska, K. J., Zhu, S., Dekkers, B. L., De Ruijter, N. C. A., Gieteling, J., & Van Der Goot, A. J. (2016b). Shear-induced structuring as a way to make anisotropic materials using soy protein concentrate. *Journal of Food Engineering*. https://doi.org/10.1016/j.jfoodeng.2016.05.010

Grabowska, K. J., Tekidou, S., Boom, R. M., & van der Goot, A.-J. (2014b). Shear structuring as a new method to make anisotropic structures from soy–gluten blends. *Foodservice Research International, 64*, 743–751.

Grabowska, K. J., Zhu, S., Dekkers, B. L., De Ruijter, N. C. A., Gieteling, J., & van der Goot, A. J. (2016a). Shear-induced structuring as a tool to make anisotropic materials using soy protein concentrate. *Journal of Food Engineering, 188*, 77–86. https://doi.org/10.1016/j.jfoodeng.2016.05.010

Jia, W., Rodriguez-Alonso, E., Bianeis, M., Keppler, J. K., & van der Goot, A. J. (2021). Assessing functional properties of rapeseed protein concentrate versus isolate for food applications. *Innovative Food Science & Emerging Technologies, 68*(February), 102636. https://doi.org/10.1016/j.ifset.2021.102636

Keppler, J. K., Schwarz, K., & van der Goot, A. J. (2020). Covalent modification of food proteins by plant-based ingredients (polyphenols and organosulphur compounds): A commonplace reaction with novel utilization potential. *Trends in Food Science & Technology, 101*(October 2019), 38–49. https://doi.org/10.1016/j.tifs.2020.04.023

Ozdal, T., Capanoglu, E., & Altay, F. (2013). A review on protein-phenolic interactions and associated changes. *Food Research International, 51*(2), 954–970. https://doi.org/10.1016/j.foodres.2013.02.009

Raheem, Z. (2014). Standard test method for tensile properties of plastics. *ASTM International, 82*(January), 1–15. https://doi.org/10.1520/D0638-14

Schreuders, F. K. G., Dekkers, B. L., Bodnár, I., Erni, P., Boom, R. M., & van der Goot, A. J. (2019). Comparing structuring potential of pea and soy protein with gluten for meat analogue preparation. *Journal of Food Engineering, 261*(May), 32–39. https://doi.org/10.1016/j.jfoodeng.2019.04.022

Schreuders, F. K. G., Schlangen, M., Kyriakopoulou, K., Boom, R. M., & van der Goot, A. J. (2021). Texture methods for evaluating meat and meat analogue structures: A review. *Food Control, 127*(April), 108103. https://doi.org/10.1016/j.foodcont.2021.108103

Tan, S. H., Mailer, R. J., Blanchard, C. L., & Agboola, S. O. (2011). Canola proteins for human consumption: extraction, profile, and functional properties. *Journal of Food Science, 76*(1), 16–28. https://doi.org/10.1111/j.1750-3841.2010.01930.x

Von Der Haar, D., Müller, K., Bader-Mittermaier, S., & Eisner, P. (2014). Rapeseed proteins-production methods and possible application ranges. *OCL - Oilseeds and Fats, 21*(1), 1–8. https://doi.org/10.1051/ocl/2013038

Wanasundara, J. P. D. (2011). Proteins of *Brassicaceae* oilseeds and their potential as a plant protein source. *Critical Reviews in Food Science and Nutrition*. https://doi.org/10.1080/10408391003749942

Wanasundara, J. P. D., McIntosh, T. C., Perera, S. P., Withana-Gamage, T. S., & Mitra, P. (2016). Canola/rapeseed protein-functionality and nutrition. *Ocl.*. https://doi.org/10.1051/ocl/2016028